The Impedance Resonance for Piezoelectric Stacks

S. Sherrit[a], S.P. Leary[a], B.P. Dolgin[a], Y. Bar-Cohen[a], R. D. Tasker[b]

[a]Jet Propulsion Laboratory, Mail Stop 82-105, 4800 Oak Grove Blvd, Pasadena, CA, 91109-8099, USA,

Email: ssherrit@jpl.nasa.gov

[b]TASI Technical Software, 11 Mack St., Unit #4, Kingston, Ontario, K7L 1N7, Canada

Abstract

A derivation of the impedance equation for a stack resonator is presented. The model is based on the effective elastic, dielectric and piezoelectric constants of the stack. The model allows for the determination of the average piezoelectric and dielectric constant of the stack material. Since the model is based on the material properties rather than circuit constants it allows for the evaluation stack performance and of specific aging or degradation mechanisms in a direct fashion.

PACS numbers: 43.38.Fx, 77.65.-j, 77.84.Dy

I. INTRODUCTION

Piezoelectric stacks are used in a variety of applications that require relatively high stress and larger strain than bulk piezoelectrics materials can produce. These include micro-positioning systems[1] solid state pumps/switches[2], noise isolation mounts[3], ultrasonic drills[4] and stacked ultrasonic transducers[5]. A variety of papers[6,7,8] have been published on fabrication and characterization of the stack using quasistatic techniques. We describe an impedance-based measurement, which can probe the state of the material properties of the piezoelectric material and determine stack performance at resonance. The measurement is non-destructive and determines the effective dielectric, elastic and piezoelectric constants of the stack. As well the model may be used to access the state of ferrroelectric/electrostrictive multilayer capacitors by inducing a piezoelectric response with a DC bias field[9].

II. THEORY

The equation for the impedance of the unbounded piezoelectric stack in the length extensional mode can be derived in a similar manner to the length extensional mode of a monolithic resonator[10]. The wave equation and the boundary conditions of a free resonator are used along with the linear equations of piezoelectricity[11] to solve for the electric displacement as a function of frequency. By assuming small field levels and traction free surfaces the voltage and current through the resonator may be calculated and the ratio used to determine the complex impedance.

Consider a piezoelectric stack of length L and area A composed of n layers of a piezoelectric material each of thickness t_P as shown in Figure 1. A bonding layer separates the piezoelectric layers of the stack, which on average is $(L/n-t_P)$ thick. The elements of the stack are connected electrically in parallel and mechanically in series. The electrodes of the stack alternate in polarity and the polarization of the piezoelectric material is aligned so that for a given applied voltage all elements expand or contract in unison depending on the polarity of the applied field as is shown in Figure 2. In order to continue with the derivation of the impedance equation we can treat the stack as a monolithic bar and determine effective material constants for the stack based on the properties of the piezoelectric elements.

II-A. Effective Properties of the Stack

The effective density of the stack is

$$\rho = \frac{\rho_P t_P + \rho_b t_b}{t_P + t_b} \tag{1}$$

The effective elastic constant governing the impedance resonance (parallel resonance frequency) is,

$$s_{33eff}^{D} = \frac{1}{4\rho f_p^2 L^2} \tag{2}$$

where f_P is the parallel resonance frequency which is the frequency at which a maximum in the resistance occurs. The effective piezoelectric constant is determined by summing the displacement for each element of the stack and is found to be.

$$d_{33eff} = n d_{33piezo} \tag{3}$$

The effective dielectric constants of the stack, if it is treated as a monolithic rod is found by noticing that each of the piezoelectric elements are electrically in parallel and the total capacitance is the sum of the capacitance of each element. The effective permittivity is calculated directly from the total capacitance and the geometry of the stack and is found to be.

$$\varepsilon^{T}_{33eff} = \frac{nL\varepsilon_{33piezo}}{t_p} \quad (4)$$

It should be noted the permittivity of the piezoelectric elements $\varepsilon_{33piezo}$ does not necessarily correspond to the free permittivity of the piezoelectric material ε^{T}_{33} since the bonding layer may reinforce the piezoelectric in the plane perpendicular to the poling direction. As a general rule the permittivity of the piezoelectric elements should be bounded by the free and clamped permittivity of the material.

The effective electromechanical coupling is then

$$\mathbf{k}_{33eff} = \frac{\mathbf{d}_{33eff}}{\sqrt{\mathbf{s}^{E}_{33eff}\varepsilon^{T}_{33eff}}} \quad (5)$$

The open circuit elastic constant for a linear piezoelectric is also related to the short circuit elastic constant. The relationship for the two constants is

$$\mathbf{s}^{D}_{33eff} = \mathbf{s}^{E}_{33eff}\left(1 - k^{2}_{33eff}\right) \quad (6)$$

The equation for the stack resonance can be derived in a similar manner as the length extensional resonator for a monolithic rod of ceramic[10]. Using effective material properties described previously, the equation governing the resonance of the stack length resonator is;

$$\mathbf{Z} = \frac{L}{\left[i\omega\varepsilon^{T}_{33eff}\left(1 - k^{2}_{33eff}\right)A\right]}\left[1 - \frac{\mathbf{k}^{2}_{33eff}\tan(\omega/4\mathbf{f}_p)}{(\omega/4\mathbf{f}_p)}\right] \quad (7)$$

where L is the length of the stack and A is the electrode area. All material constants excluding the geometric and density terms can be treated as complex to account for phases shifts due to losses in the material constant. The analysis of the material constants for the stack length resonator mirrors the analysis of the length extensional resonator. The complex parallel frequency constant found in the equation for impedance is determined by equation 1, which is a function of the length L, density ρ, and the effective open circuit elastic compliance. It should be noted that the elastic constant shown in equation 2 is an effective elastic constant for the piezoelectric elements and the bond layers. The elastic constant of the bond material can be estimated by using the determined value of the effective compliance, the elastic constant of the piezoelectric material (assumed to be known) and the equation for the effective elastic constant .in terms of the elastic constants and density of the layers. In the piezoelectric stack the thickness of the bond layer is usually much smaller than the piezoelectric element thickness and as an approximation it is sufficient to use the density of the piezoelectric material in equation 2.

II-B. Limitations of Model

The impedance measurement is a small signal excitation of the stack resonator however in the majority of applications where a stack is used the sample is driven at high fields and low frequencies. The degree to which the small signal measurement agrees with data from quasi-static high field measurements depends primarily on whether the material is hard (large coercive field) or soft (small coercive field)[12]. For a material which is soft the dielectric and piezoelectric constant are found to depend linearly on the size of the drive field up to the coercive field where domains begin to switch[13]. For example for the Motorola 3203HD material both the piezoelectric and dielectric constant were found to be double the small signal values at fields approaching the coercive field of the material. For harder materials the field dependence is less pronounced. A similar dependence is found for piezoelectric ceramics under pre-stress[14].

In addition, the stack resonator measurement at low signals strength is isothermal while in many applications a temperature increase in the stack is measured due to the dissipation of mechanical and electrical energy during operation. In general the temperature dependence of the dielectric and the piezoelectric constant is again related to the coercive field. For low coercive field materials the Curie temperature is typically closer to room temperature which means the peak in the dielectric properties as a function of temperature is nearer the operating temperature. The closer the room or operating temperature is to this peak the larger the change in the permittivity for a given temperature change. This suggests that for both these effects the larger the coercive field the better the agreement between the small signal properties and the properties determine at operating conditions

Another possible limitation of the small signal measurement is the frequency of measurement. For quasi-static devices which operate at low frequency the permittivity and piezoelectric constant are slightly higher at low frequencies due to an intrinsic dispersion in the materials properties as the result of domain wall motion.

In summary, with reference to the limitations discussed above, it is apparent that the small signal resonance measurement is in effect a baseline measurement which allows for the investigation of the stack material parameters in the linear reversible regime under isothermal conditions

III. EXPERIMENTAL

The impedance spectra for a set of well-aged Morgan Matroc stacks (5mm x 5mm x 5mm) (PZT 4S) were measured using a Solartron 1260 impedance analyzer. Impedance spectra of the stack leads were taken to determine the short circuit corrections for the holder and leads. The number of layers was determined with an optical microscope. The effective density was determined by removing the leads of one of the stacks and measuring the mass of the stack and dividing the stack volume. These values are shown in Table 1. It should be noted that these stack samples differ from an ideal stack in that they have a small aspect ratio (1:1), contain endcaps (0.6mm PZT), and the internal electrodes are discontinuous and do not cover the full cross sectional area of the stack.

III-A Short Multilayered Stack

The stack impedance resonance spectrum is shown in Figure 3 for one of the short Morgan Matroc stacks. The first major resonance is the length extensional resonance of the stack. Although the width and length are the same size for this set of stacks the width and length resonance modes are shifted away from each other due to the anisotropy of the piezoelectric ceramic and the increase in compliance, due to layering, in the length direction. Both of these effects act to shift the length extensional resonance to a lower frequency than the lateral mode resonance, which are identified by the smaller resonances above f_p. The spectra was fit using Smits' [15] method with the Piezoelectric Resonance Analysis Program PRAP[16]. The fit is seen to be very good over the frequency range shown with small deviations likely due to frequency dispersion in the material properties. The values of the effective material constants for the fit shown in Figure 3 are listed in Table 2. The mechanical Q for the resonator can be found by dividing the real elastic compliance s^D by the imaginary component. The dielectric dissipation tanδ is the imaginary component of the free permittivity divided by the real value.

The effective piezoelectric constant is a measure of the strain per electric field or the displacement per volt applied to the stack.

$$d_{33eff} = \Delta S / \Delta E = \Delta L / \Delta V \tag{8}$$

Using the effective piezoelectric coefficient in Table 2. We see that for a 100 volt signal on the stack the stack would displace 0.88 microns. The compares to 0.90 μm as can be calculated from the manufacturers literature. The stack capacitance and electrical dissipation are found to be 38.5 nF and -0.006. The mechanical Q is found to be 410. Using equations 3 and 4 and the data in Tables 1 and 2, we can calculate the effective piezoelectric and dielectric constant of the material in the stack. The results along with the material properties, as measured by the manufacturer[17], are shown in Table 3.

The analysis was performed on a set of 5 stack resonators and the average and percent standard deviation for the real component of the material constant is shown in Table 4. The standard deviation of the imaginary components were found to be much larger and on the order of 50%. Much of this spread in values is thought to be due to the noticeable dispersion in the dissipation and the measurable variance in the dispersion from stack to stack. The percent standard deviation in the real values of the material constants is of the same order as that found for monolithic bulk ceramic resonators.

III-B Long Potted Monolithic Stack

The measurement and analysis were repeated for longer multilayer stacks. The geometry was similar to the sample geometry shown in Table 1. except the stacks were 10 mm long and the stack was coated with a loctite/rubber/loctite layer. After testing the polymer layers were removed and the sample was re-measured. The properties did not change. The stack was examined under a microscope and it was noticed that the electrode edge could not be seen in the sides of the stack which, did not have the solder pad. This suggests that an additional inactive area that was not present in the short stacks. According to the manufacturer the internal electrode area was reduced by the same amount as with the short stacks by the offset in the internal electrodes and electrode patterning. The stack is comprised of 65 piezoelectric layers and inactive endcaps which are 0.5mm - 0.6 mm thick. The resonance spectra are shown in Figure 4. The parameters determined from the analysis of the data are shown in Table 5.

The effective dielectric constant of the piezoelectric material in the long stack was found to be 1500 and the dissipation was found to be 0.012. The mechanical Q is 180 The piezoelectric constant was determined to be 215 pC/N which is considerably less than the d_{33} determined for the short stack. A quasistatic high field measurement performed by the manufacturer prior to shipping found the piezoelectric constant of the material to be (dS/dE)/n = 265 pC/N which is a 10-15% reduction from the nominal value of 300 pC/N for the long stacks[18].

The discrepancy between the resonance value and the quasistatic measurement was of the order of 20% for the long stack. The decrease in d_{33} is primarily associated with the decrease in the electromechanical coupling k_{33}. It should also be noted that the longer stack is stiffer and the mechanical Q is smaller by a factor of two. The decrease in the measured value of the piezoelectric and coupling coefficient determined from resonance is likely due to edge pinning by the inactive margins which appears to be more significant at resonance.

IV. CONCLUSIONS

A model for the impedance resonance of a stack resonator was presented which allowed for non destructive evaluation of the stack performance. The stack resonator model allowed for the determination of an effective elastic, dielectric, piezoelectric and coupling constant from complex impedance spectra. A set of multilayer stack resonators with a small inactive region were tested and the material constants controlling the impedance spectra were determined using the model. The constants were found to be in good agreement with the data presented by the manufacturers. In the case of resonators with embedded electrodes that had inactive margins, which were mechanically connected, the model was found to produce a good fit to the data. However a reduction in the effective piezoelectric coefficient was measured due to the clamping by the inactive margins.

V. ACKNOWLWDGEMENTS

The research at Jet Propulsion Laboratory (JPL), California Institute of Technology, was carried out under a contract with National Aeronautics Space Agency (NASA). The results reported in this manuscript were obtained under a TRIWG task, Code S, Mr. David Lavery and Dr. Chuck Weisbin are the Managers of TRIWG.

VI. REFERENCES

[1] Michael Goldfarb, Nikola Celanovic, "Modeling Piezoelectric Stack Actuators for Control of Micromanipulation" , IEEE Control Systems MAG 17: (3) 69-79 JUN 1997

[2] S. Mitsuhashi, K. Wakamatsu, Y. Aihara, N. Okihara, "Relay Using Multilayer Piezoelectric Actuator", Jpn. J. of Appl. Phys. **24** Supp. 24-3, pp. 190-192, 1985

[3] S.A. Wise, M.W. Hooker, Characterization of Multilayer Piezoelectric Actuators for use in Active Isolation Mounts", NASA Langley, NASA Technical Brief - 4742, March, 1997

[4] Cybersonics Inc. , 5368 Kuhl Road, Erie, PA 16510

[5] D.J. Powell, G. Hayward, R.Y. Ting ,"Unidimensional modeling of multi-layered piezoelectric transducer structures", IEEE Trans On Ultrasonics Ferroelectrics and Frequency Control, **45**: (3) pp.667-677, May, 1998

[6] S. M. Pilgrim, A.E. Bailey, M. Massuda, F.C. Poppe, A.P. Ritter, " Fabrication and Characterization of PZT multilayer actuators, Ferroelectrics, **160,** pp. 305-316, 1994

[7] L.S. Bowen, T. Shrout, W.A. Shulze, " Piezoelectric Properties of Internally Electroded PZT Multilayers", Ferroelectrics, **27**, pp.59-62, 1980

[8] B. Zickgraf, G.A. Schneider, F. Aldinger, " Fatigue Behavior of Multilayer Piezoelectric Actuators", Proceedings of the 9th International Symposium on the Applications of Ferroelectrics, University Park, Pennsylvania, pp 325-328, 1994

[9] Ousten Y, Mejdi S, Bechou L, Tregon B, Danto Y, "Comparison between piezoelectric method and ultrasonic signal analysis for crack detection in type II multilayer ceramic capacitors, Quality And Reliability Engineering International, **14**: (2) pp.91-94 ,1998

---

[10] D. A. Berlincourt, D.R. Curran, H. Jaffe, “Chapter 3- Piezoelectric and Piezomagnetic Material and their Function in Transducers, pp. 169-270, Physical Acoustics-*Principles and Methods,* Volume 1-Part A, ed. W.P. Mason Academic Press, New York, 1964

[11] IEEE Standard on Piezoelectricity IEEE/ANSI Std. 176, 1987

[12] D.A. Berlincourt, H.H.A. Krueger, "Domain Processes in Lead Titanate Zirconate and Barium Titanate Ceramics", J. Appl. Phys., **30**, (11), pp. 1804-1810, 1959

[13] S. Sherrit, H.D. Wiederick, B.K. Mukherjee, M. Sayer "Field dependence of the complex piezoelectric, dielectric, and elastic constants of Motorola PZT 3203 HD ceramic", Proc. SPIE Vol. 3040, p. 99-109, Smart Structures and Materials 1997: Smart Materials Technologies, Wilbur C. Simmons; Ilhan A. Aksay; Dryver R. Huston; Eds.

[14] R.F. Brown and G.W. McMahon "Material Constants of Ferroelectric Ceramics at High Pressure", Can. J. Physics, **40**, pp.672-674, 1962

[15] J.G. Smits, " Iterative Method for Accurate Determination of the Real and Imaginary Parts of Materials Coefficients of Piezoelectric Ceramics, IEEE Trans on Sonics and Ultrasonics, (SU-23),(6), pp. 393-402, November, 1976

[16] PRAP, Piezoelectric Resonance Analysis Program, TASI Technical Software, 174 Montreal St. Kingston, ON, Canada, K7K 3G3, http://www.canlink.com/tasi/tasi.html

[17] Monolithic Multilayered Actuators", Page insert produced by Morgan Matroc, 232 Forbes Road, Bedford, Ohio, 44146 USA, http://www.morganmatroc.com/

[18] Alan Metcalfe, Morgan Matroc, Private communication

List of Tables

Property	Value
Length (L)	0.00501 m
Electrode Area (A)	0.0000162 m^{2*}
Width 1 (w)	0.00505 m
Width 2 (d)	0.00501 m
Density (ρ)	7794 kg/m^3
No of elements (n)	28
Thickness of elements (t_P)	0.000135m

*Estimated from overlapping length of the top and bottom electrodes and taking into account herringbone pattern on electrodes.

Table 1 -Sherrit et. al. - JASA

Property	**Real**	**Imaginary**
s^D_{33eff} (m^2/N)	1.28x10^{-11}	-3.1 x10^{-14}
ε^T_{33eff} (F/m)	1.25x10^{-5}	-9.0 x10^{-8}
d_{33eff} (C/N)	8.80x10^{-9}	-4.9 x10^{-11}
k_{33eff}	0.572	-0.00032

Table 2 -Sherrit et. al. - JASA

Property	Resonance Value (Effective values)	Manufacturers Specifications Short stacks
d_{33} (pC/N)	320	330
K^T_{33eff}	1507	1500

Table 3 -Sherrit et. al. - JASA

Property	Real value (%Std D)
s^{D}_{33eff} (m^2/N)	1.29 x10^{-11} (0.9%)
ε^{T}_{33eff} (F/m)	1.35 x10^{-5} (6.5%)
d_{33eff} (C/N)	9.0 x10^{-9} (4.7%)
k_{33eff}	0.575 (2.3%)

Table 4 -Sherrit et. al. - JASA

Property	**Real**	**Imaginary**
s^{D}_{33eff} (m^2/N)	1.16 x10^{-11}	-6.3 x10^{-14}
ε^{T}_{33eff} (F/m)	6.24 x10^{-5}	-7.3 x10^{-7}
d_{33eff} (C/N)	1.36 x10^{-8}	-1.8 x10^{-10}
k_{33eff}	0.453	-0.0017

Table 5 -Sherrit et. al. - JASA

List Of Figures

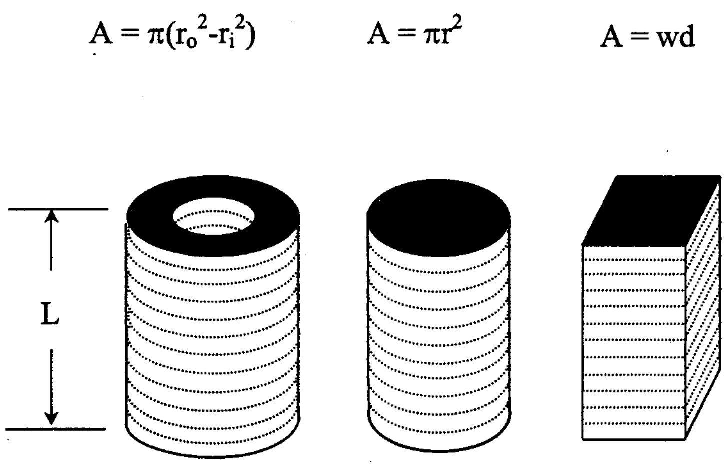

Figure 1 - Sherrrit et. al. - JASA

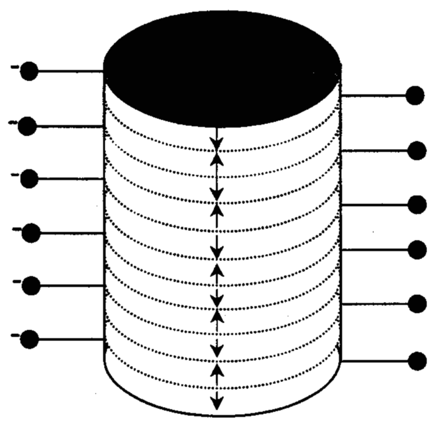

Figure 2 - Sherrrit et. al. - JASA

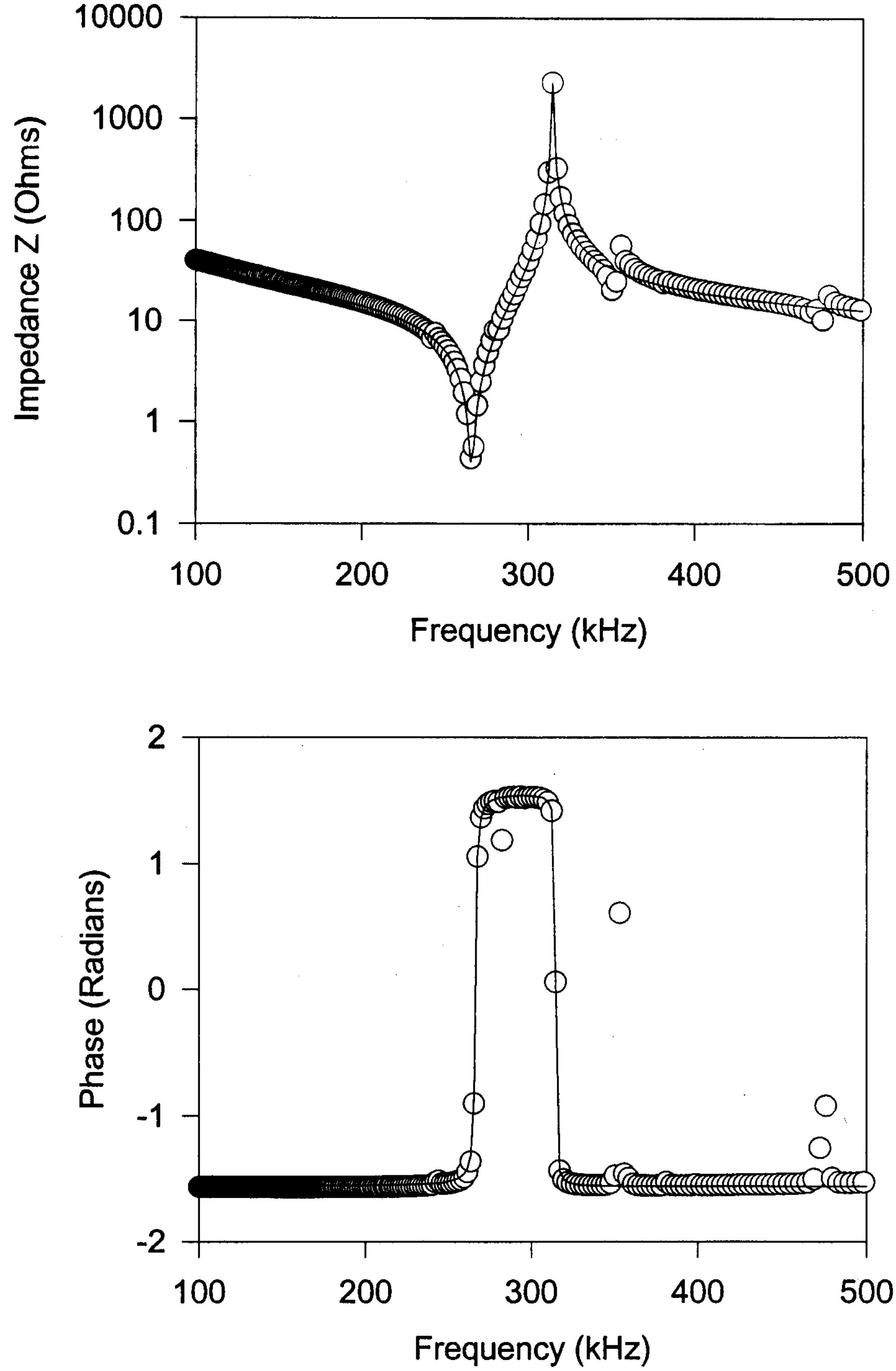

Figure 3 - Sherrit et. al. JASA

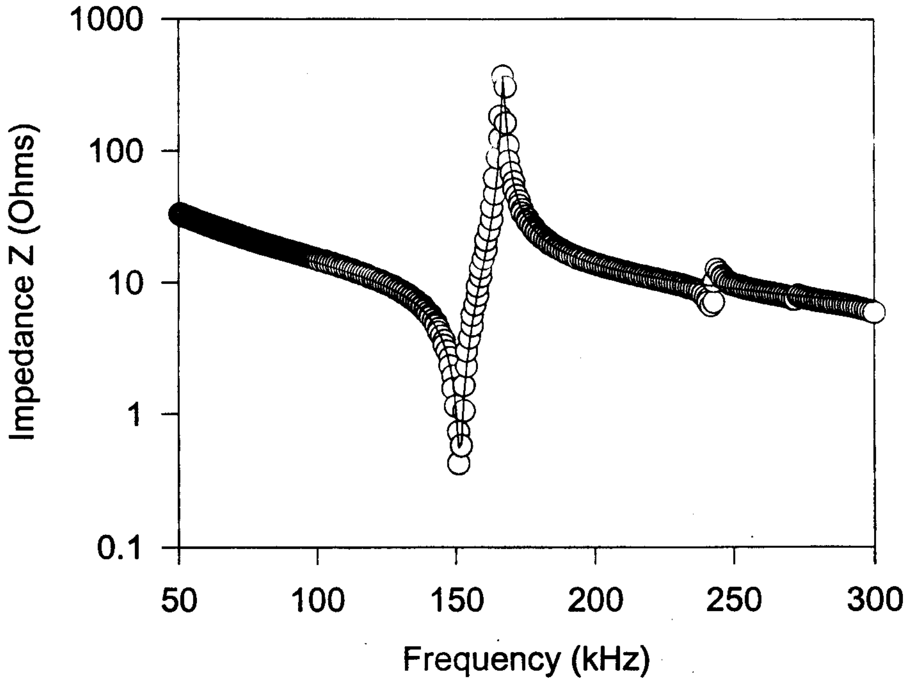

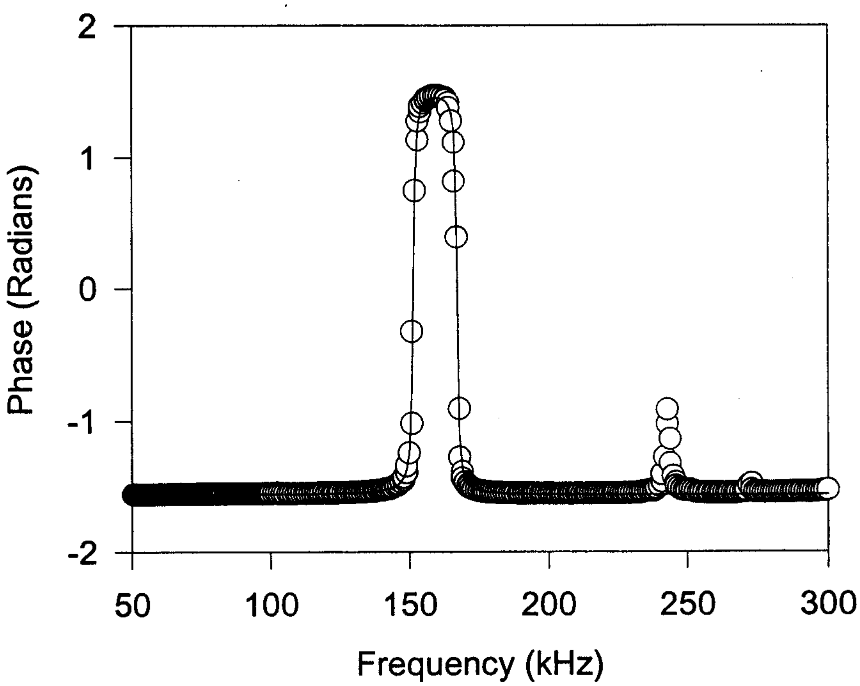

Figure 4 - Sherrit et. al. JASA